Experimental and theoretical band-structure studies of refractory metal silicides

J. H. Weaver

Synchrotron Radiation Center, University of Wisconsin-Madison, Stoughton, Wisconsin 53589

V. L. Moruzzi

IBM Thomas J. Watson Research Center, Yorktown Heights, New York 10598

F. A. Schmidt

Ames Laboratory, U. S. Department of Energy, Ames, Iowa 50011

The electronic structures of bulk refractory metal disilicides VSi_2, $TaSi_2$, and $MoSi_2$ have been examined using photoelectron spectroscopy with synchrotron radiation. Photoelectron energy distribution curves measured for $9 \leq h\nu \leq 140$ eV show occupied bands (full width $\simeq 12$ eV) dominated by metal d-derived states within 3–4 eV of E_F and by Si $3s$- and $3p$-derived features at higher binding energies. The V $3p$, Mo $4p$, Ta $5p$, Ta $4f$, and Si $2p$ core-emission features are also shown. Self-consistent band calculations for a series of cubic silicides MSi_3, MSi, and M_3Si (M denotes V or Mo) predict dominant metal d character within 5 eV of E_F, Si s states centered at about -10 eV, Si p states centered near -5 eV, and substantial M-Si hybridization, in agreement with experiment.

INTRODUCTION

There is a great deal of interest in the interface between a transition-metal silicide and silicon.[1-8] Much of this interest is related to the technological importance of these Schottky barriers and their use in electronics devices. Within the last few years major progress has been made toward understanding the electronic structure of several silicide-Si interfaces. Recent attention has focused on the junction itself and the dynamics involved in forming a junction *in situ*, e.g., by metal deposition on Si followed by thermal treatments to form a thin silicide overlayer. Remarkably, there have been no studies until now of the electronic structure of bulk silicides; only the amorphous Pd-Si glasses[9-11] have been examined.

Experimental and theoretical studies of bulk silicides identify the roles of the metal and silicon in the band structure, reveal the metal-silicon mixing or hybridization, and contribute to the understanding of chemical bonding. Further, by identifying the electronic properties of the bulk silicide, it becomes possible to distinguish between bulk silicide properties and intrinsic interface properties and ultimately understand the interface evolution from silicon metal to silicon silicide metal.

In this paper, we present the results of a photoelectron spectroscopy study of three representative refractory metal disilicides, VSi_2, $TaSi_2$, and $MoSi_2$. The photoemission measurements, conducted with synchrotron radiation, reveal trends in the three related body-centered-tetragonal disilicides. Total and l-decomposed densities of states were calculated for a series of V-Si and

Mo-Si compounds in the Cu_2Au and $CuAu$ structures in order to serve as a guide in the interpretation of observed features in the disilicide spectra. The calculations offer important insight into the band structure of silicides, including the dependence on the atomic ratio of M to Si. The combined experimental and theoretical studies allow us to identify the band-structure regions where the metal-derived states and the silicon-derived features are most important. These results help us understand the physics of silicides; it will remain for later calculations to examine the details of the specific silicide.

EXPERIMENTAL AND THEORETICAL TECHNIQUES

Samples of the bulk disilicides of V, Mo, and Ta were prepared by arc melting the high-purity constituents in a nonconsumable arc furnace on a water-cooled copper hearth.[12] The materials (~50 g) were melted under a purified Ar atmosphere using a water-cooled tungsten tip electrode (straight polarity, approximately 300 A). The resulting buttons were flipped and remelted at least five times to ensure homogeneity. Samples were cut for metallographic examination and for metal analysis. Optical metallographic examination showed grains up to ~1×4 mm. VSi_2 and $TaSi_2$ samples, when polished and electropolished (12% by volume sulfuric acid in methanol at 200 K) and viewed under 320 magnification, were essentially single phase. $MoSi_2$ had slight amounts of intragranular second phase that appeared bluish against the grey silicide matrix background. Such second-phase effects are insignificant as concluded, for

2916
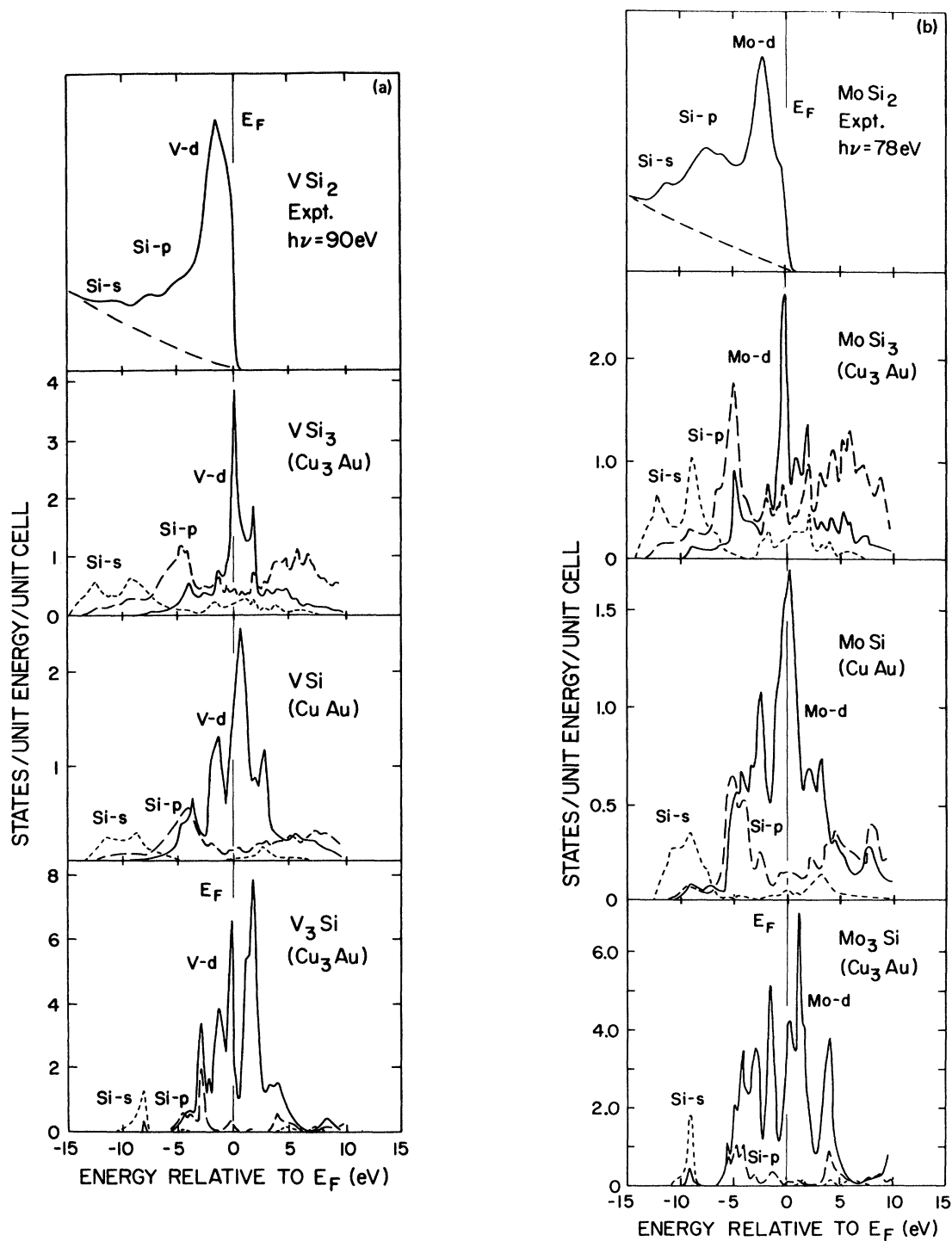
FIG. 1. (a) Comparison of an experimental photoelectron energy distribution curve for VSi_2 with l -projected state densities for V_3Si (Cu_3Au structure), VSi (CuAu structure), and VSi_3 (Cu_3Au structure). The theoretical partial-state densities were calculated using the augmented-spherical-wave method developed by Williams, Kubler, and Gelatt. The calculations predict, and the experiment confirms, that the primary character of the states within ~ 5 eV of E_F are metal d derived. The deeper lying bands are primarily $3s$–$3p$ derived. (b) Results for Mo–Si analogous to those of VSi [see (a)].

example, by examining the Si $2p$ core emission (see Fig. 1 and discussion below).

The disilicides of V, Ta, and Mo are brittle and they fracture easily; they are also hard and are highly resistant to chemical attack even at elevated temperatures. This last property has made several of the refractory silicides attractive in technological applications. These disilicides have high melting points, low vapor pressures, and are relatively easy to prepare in bulk form. The silicides of V and Ta crystallize in the $CrSi_2$ C40 structure. The $MoSi_2$ crystal structure is body-centered-tetragonal (C1 1b structure type, $MoSi_2$ structure).[13]

All measurements were performed in a bakeable, ultrahigh-vacuum photoelectron spectroscopy system (base pressure 3×10^{-11} Torr, operating pressures for these runs was $4-5 \times 10^{-11}$ Torr). The arc-melted buttons were cut to give posts ~$2 \times 3 \times 10$ mm^3 which were mounted onto copper sample holders.[14] These were loaded onto a bank having a capacity of ~20 for extended runs. Before the measurements, samples were removed from

the bank with an x-y-z-ϕ-flip-tilt manipulator. fractured *in situ* with a sharpened tungsten cleaving tool, and positioned at the common focus of the monochromatic radiation beam and the electron energy analyzer. Several cleaves could usually be made with each post. A detailed discussion of the geometry of the systems can be found in Ref. 15. The radiation was monochromatized with a 3 m toroidal grating monochromator after being emitted by orbiting electrons in the 240-MeV electron storage ring Tantalus at the University of Wisconsin-Madison. Photoelectron energy distribution curves were measured in photon energy increments of 1–2 eV for $9 \leqslant h\nu \leqslant 90$ eV with overall resolution (electrons plus photons) of about 0.4 eV. The Si $2p$ core levels were studied at $h\nu = 140$ eV.

The energy-band calculations are based on the local-density approximation to electronic exchange and correlation effects and on the augmented-spherical-wave (ASW) procedure for the solution of the effective one-electron equations. The ASW method developed by Williams, Kubler, and Gelatt is the spherical-wave analog of Slater's aug-
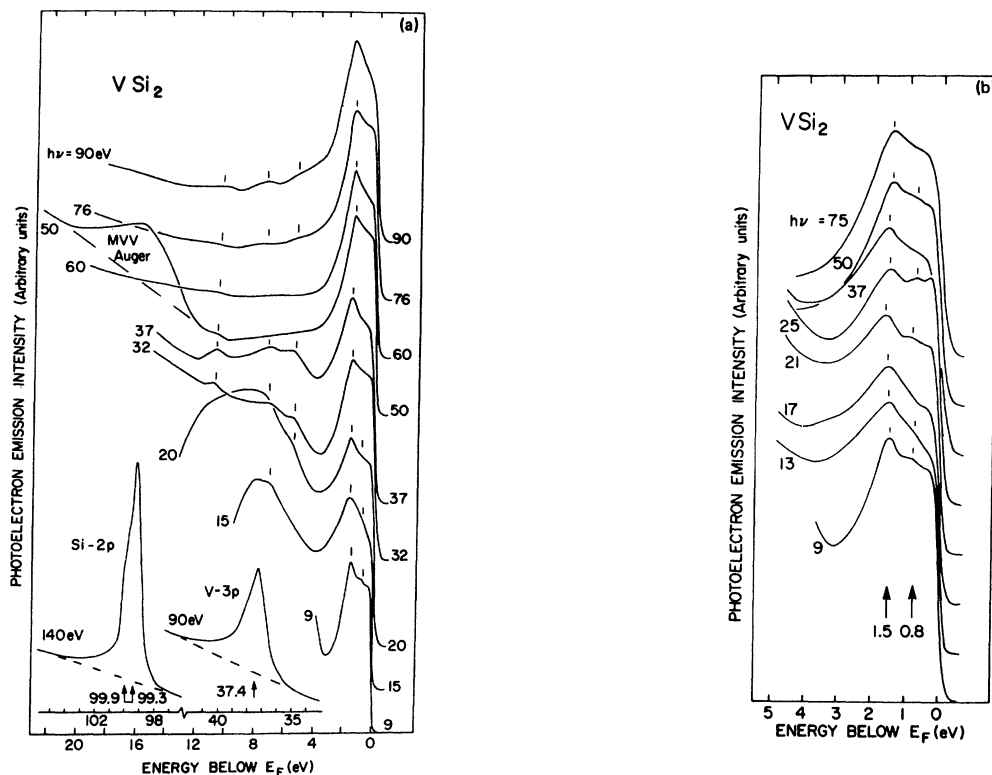
FIG. 2. (a) Photoelectron energy distribution curves for VSi$_2$ showing predominantly d-derived bands within ~3 eV of the Fermi level E_F and the deeper-lying Si-derived bands. Auger emission can be seen at $h\nu = 50$ eV (full width approximately 9 eV); at lower photon energies, it overlaps and obscures direct emission features. (b) A collection of energy distribution curves for VSi$_2$ showing the initial-state features in the d-derived bands near E_F. The dominant feature falls at 1.5–1.6 eV below E_F and a weaker structure can be seen at about -0.8 eV. No dispersion of these is observed and they are identified as density-of-states features.

mented-plane-wave (APW) method and is closely related to Andersen's linear combination of muffin-tin orbitals (LMTO) method.[16] The calculations are self-consistent (calculated electronic charges for successive iterations agree to within 0.001 electrons within the Wigner-Seitz sphere), parameter free (the only inputs were the atomic numbers and the structure type), and correspond to theoretical equilibrium (the atomic spacing was systematically varied until the total energy was minimized).

RESULTS AND DISCUSSION

The calculated l-decomposed density of states for VSi_3 (Cu_3Au crystal structure), VSi (CuAu), and V_3Si (Cu_3Au) are shown in Fig. 1(a). The analogous results for the Mo-Si compounds are shown in Fig. 1(b). The different scales for the theoretical results reflect the different numbers of atoms (and electrons) per unit cell. For each series of calculations, we find the silicon s states centered at approximately -10 eV, the silicon p states centered at approximately $4-5$ eV below E_F, and the metal d states near E_F and extending down to -5 eV. Calculations for VSi and MoSi with the CsCl crystal structure show the d character more strongly peaked near E_F (~2 eV of E_F) but with approximately the same overall width (~5 eV). As shown in Fig. 1, the widths of the Si $3s$ and Si $3p$ derived bands increase with increasing Si content and they shift to somewhat higher binding energy. Although calculations of the disilicide (CaF_2) were beyond the present scope of our computer codes, we expect the density-of-states features to be qualitatively similar to those shown. Also shown in Figs. 1(a) and 1(b) are photoelectron energy distribution curves for VSi_2 and $MoSi_2$, respectively, measured with photon energies of 78 eV, i.e., sufficiently high that density-of-states features are emphasized.

Photoelectron energy distribution curves measured for VSi_2 are shown in Fig. 2(a) for $9 \leqslant h\nu \leqslant 140$ eV. The dominant feature within ~3 eV of E_F reflects the V-derived d character and the Fermi level falls in a region of high, but diminishing, state density. The d-band peak at -1.6 eV is seen for all photon energies and a relatively weak feature is visible at about -0.8 eV [better seen in Fig. 2(b)]. The calculated density of states supports the association of the dominant feature with the V-derived d bands even though the experimental details are not reproduced in detail.

Structure below the d bands can be associated with the Si-derived s and p bands. Features in those bands are better seen at some photon energies than at others. For $h\nu = 37$ eV, the mini-

mum between the d bands and the Si-derived bands falls ~4 eV below E_F, and there are maxima at -5.5, -7.2, and -10.4 eV. For lower photon energies the background from inelastically scattered secondaries obscures the Si-derived features; e.g., only the features at -5.5 and -7.1 eV can be identified with complete confidence for $h\nu = 20$ eV. The total width of the Si-V valence-band emission is ~12 eV as predicted by the VSi or VSi_3 calculations.

In Fig. 2(a) for $h\nu = 50$ eV, we show Auger emission (MVV) arising from the V $3p$ cores (binding energy 37.4 eV). For lower photon energies ($37 \leqslant h\nu \leqslant 50$ eV including the He resonance line at 40.8 eV), the Auger feature overlaps the valence-band direct emission.

In Fig. 2(a), we show the Si $2p$ doublet, the line shape of which is consistent with a spin-orbit splitting of 0.6 eV.[17] From a deconvolution of the $2p$ structure, we identify the binding energies to be 99.3 and 99.9 eV for the $2p_{1/2}$ and $2p_{3/2}$ levels, respectively, referenced to the Fermi level.

Examination of the Si $2p$ feature shown in Fig.
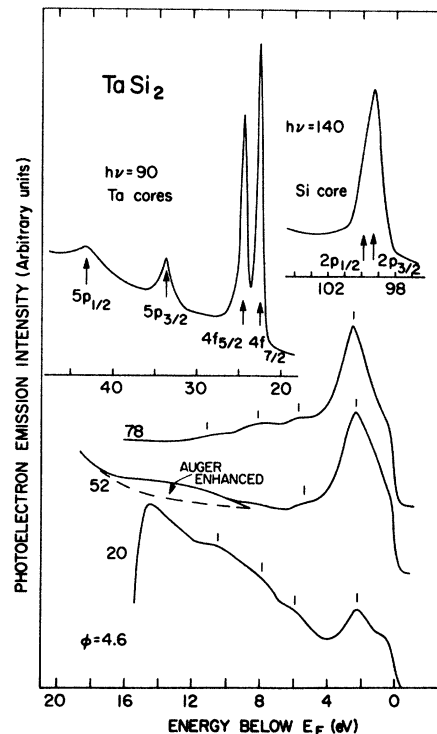
FIG. 3. A collection of energy distribution curves for $TaSi_2$ showing spectra very similar to those for VSi_2. The d bands are wider, but the overall character remains the same. The core-level emission from the Ta $4f$ doublet and $5p$ doublet is shown in the top of the figure together with the Si $2p$ portion of the spectrum taken at $h\nu = 140$ eV.
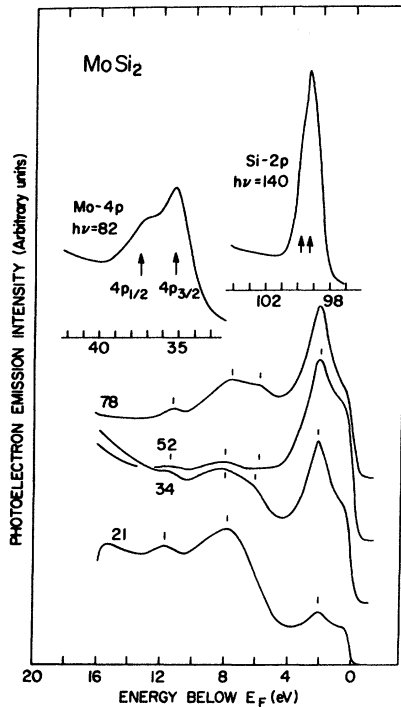
FIG. 4. A collection of energy distribution curves for MoSi$_2$. The prominent features near E_F are interpreted as d derived while the deeper features reflect Si-derived bands. Core-level features from Mo and Si are shown at the top of the figure.

FIG. 5. A comparison of energy distribution curves for VSi$_2$, TaSi$_2$, and MoSi$_2$. The d bands of VSi$_2$ are narrower than those of either MoSi$_2$ or TaSi$_2$ and the density of states at E_F is higher, as judged by the strength of the emission at the trailing edge of the Fermi cutoff. Features within the Si p-derived bands are relatively independent of the metal contribution in these disilicides. The $4s$ band at approximately -11 eV is also unchanged in general appearance.

2(a) indicates that Si is present only in a single charge state. Oxide contamination would introduce a second feature shifted toward higher binding energy. The presence of a second phase or of elemental Si at the surface would tend to broaden the Si 2p feature (at $h\nu = 140$ eV the kinetic energy of the exc"ed electron is ~40 eV, the escape depth of the electron is only ~5 Å). The full width at half maximum (~1.1 eV) is consistent with what has been observed for Si in angle-resolved photoemission studies of V$_3$Si (Ref. 18), also using a 3 m toroidal grating monochromator (the resolution of our measurements is limited primarily by the resolution of the monochromator, ~0.6 at $h\nu = 140$ eV).

In the overview figure for VSi$_2$ [Fig. 2(a)], we also show the V 3p core emission structure as measured with $h\nu = 90$ eV. The binding energy shown is 37.4 ± 0.2 eV, compared to 37.2 ± 0.2 eV for elemental V (Ref. 19) or 37.1 eV for vanadium in V$_3$Si.[18]

An expanded energy view of the initial states of VSi$_2$ within ~5 eV of E_F is shown in Fig. 2(b). Two well-defined structures can be identified in the VSi$_2$ d bands at 1.5–1.6 eV and ~0.8 eV below E_F. These features do not disperse with photon energy, although they do vary in relative strength.

As shown in Fig. 2(a), emission from the Si-

derived s- and p-states is low at energies of 50–60 eV but is greater at higher photon energies and the d bands remain prominent for all photon energies. In part this is an artifact of the normalization of the spectra since the spectra have been normalized to keep the d-band intensity approximately constant.

In order to identify trends and to support our interpretation of the spectra for VSi$_2$, we have extended the measurements to include bulk samples of TaSi$_2$ and MoSi$_2$ as shown in Figs. 3 and 4, respectively. In Fig. 5 we compare the three metal disilicides. For VSi$_2$, the width of the d-derived band is considerably narrower than in isoelectronic TaSi$_2$ or in MoSi$_2$. The peak in the d bands shifts from about -1.6 eV in VSi$_2$ to about -2.4 eV in TaSi$_2$ and about -2.2 eV in MoSi$_2$. At the same time, the Si-derived features have shifted very little, a trend supported by the MoSi calculations of Fig. 1(b). The Si 3s states fall at approximately -11 eV for all three silicides and the two features in the Si p bands occur at roughly 5.8 and 7.5–8 eV below E_F. Comparison of the three spectra of Fig. 5 suggests that the density of states at E_F is higher in VSi$_2$ than in either TaSi$_2$ or MoSi$_2$ as indi-

cated by the relative heights of the dominant peak and the trailing edge of the Fermi-level cutoff. To our knowledge, however, there have been no heat capacity measurements which could support this preliminary observation.

Core-level spectra for $TaSi_2$ and $MoSi_2$ are also shown in Figs. 3 and 4. From Fig. 3 it can be seen that the Ta $4f$ levels have binding energies of 22.5 and 24.4 eV (spin-orbit splitting of 1.9 eV), compared to 21.57 and 23.48 ±0.05 eV for bulk $4f$ level in single crystal Ta.[20] The Ta $5p_{1/2}$ binding energy is 33.5 eV and that of the $5p_{3/2}$ is 42.4 eV (splitting 8.9 eV). For $MoSi_2$, the $4p_{3/2}$ core has a binding energy of 35.2 eV and the spin-orbit splitting is approximately 2.1 eV.

CONCLUSIONS

We have found that the electronic structure of the refractory metal silicides VSi_2, $MoSi_2$, and $TaSi_2$ is dominated by metal d-derived character within ~5 eV of the Fermi level and that the Si s- and p-derived bands extend to ~12 eV below E_F. We have observed that the d bands are wider for $TaSi_2$ than VSi_2, as was expected. Our interpretation of the observed features according to Si-sp or metal-d character is supported by self-consis-

tent calculations of the total and l-projected density of states.

The l-decomposed state densities provide a clue to understanding the chemical bonding in these compounds. As in the case of Pd silicides,[21] strong interactions between metal-d and silicon-p states lead to the formation of hybridized bonding and anti-bonding complexes. The bonding complex, pinned at the lower edge of the metal-d band, is completely occupied. The antibonding complex is usually diffused (except for the case of the metal-rich compounds) and well above E_F.

ACKNOWLEDGMENTS

---

[1] We will not attempt an exhaustive review of the literature of Schottky barriers but refer the reader to the 107 references for III-V compounds cited by I. Lindau, P. W. Chye, C. M. Garner, P. Pianetta, C. Y. Su, and W. E. Spicer, J. Vac. Sci. Technol. 15, 1332 (1978). References 7–38 deal with theoretical treatments of interfaces; other references discuss experimental results.

[2] See S. M. Sze, *Physics of Semiconductor Devices* (Wiley, New York, 1969); A. G. Milnes and D. L. Feucht, *Heterojunctions and Metal-Semiconductor Junctions* (Academic, New York, 1972); V. L. Rideout, Solid State Electron. 18, 541 (1975).

[3] G. Margaritondo, J. E. Rowe, and S. B. Christman, Phys. Rev. B 14, 5396 (1976).

[4] J. L. Freeouf, G. W. Rubloff, P. S. Ho, and T. S. Kuan, Phys. Rev. Lett. 43, 1836 (1979).

[5] J. M. Andrews and J. C. Phillips, Phys. Rev. Lett. 35, 56 (1975).

[6] I. Abbati, L. Braicovich, and A. Franciosi, Solid State Commun. 33, 881 (1980); L. Braicovich, C. M. Garner, P. R. Skeath, C. Y. Chye, I. Lindau, and W. E. Spicer, Phys. Rev. B 20, 5131 (1979).

[7] J. L. Freeouf, Solid State Commun. 33, 1059 (1980).

[8] J. M. Poate, J. E. Rowe, and K. C. R. Chiu, Bull. Am. Phys. Soc. 25, 266 (1980) reported low-energy electron diffraction (LEED) studies of Pd_2Si and $NiSi_2$; and J. E. Rowe, private communication.

[9] J. D. Riley, L. Ley, J. Azoulay, and K. Terakura, Phys. Rev. B 20, 776 (1979).

[10] P. Oelhafen, M. Liard, H.-J. Güntherodt, K. Berresheim, and H. D. Polaschegg, Solid State Commun. 30, 641 (1979).

[11] B. S. Waclawski and D. S. Bondreaux, Solid State Commun. 33, 589 (1980).

[12] Spark source mass spectrometric analysis gave the following impurities in parts per million atomic: For V-Si, Al(100), Ca(2), Fe(20), Mo(16), Ni(10), Ta(4), Ti(2), W(<2), Zn(1); for Ta-Si, Ca(4), Fe(2), Mo(3), Ti(2), W(14), Zr(5); for Mo-Si, Cr(2), Fe(15), Ni(3), V(<10), W(130). Carbon impurity levels were identified with combustion chromatography; nitrogen and oxygen impurities were determined by vacuum fusion analysis as follows (ppm-atomic): V-Si, C(40), N(160), and O(4); Ta-Si, C(150), N(140), and O(160); Mo-Si, C(1400), N(100), and O(14). Other impurity levels were less than 1-ppm atomic. Si-to-metal ratios were determined to be [Si]/[V]=2.05, [Si]/[Ta]=2.18, and [Si]/[Mo]=2.01. Attempts to grow large-grained (~cm) single crystals by both a direct current arc and an induction melting technique were unsuccessful.

[13] B. Aronsson, T. Lundström, and S. Rundqvist, *Borides, Silicides, and Phosphides, A Critical Review of their Preparation, Properties, and Crystal Chemistry* (Wiley, New York, 1965). Literature values for the lattice constants are as follows: VSi_2 $a=4.571$, $c=6.372$, $TaSi_2$ $a=4.783$, $c=6.565$, $MoSi_2$ $a=3.202$, $c=7.852$.

[14] A picture of the experimental arrangement can be seen on the cover of Science 206, (1979) No. 4415.

[15]G. Margaritondo, J. H. Weaver, and N. G. Stoffel, J. Phys. E $\underline{12}$, 662 (1979).

[16]A. R. Williams, J. Kubler, and C. D. Gelatt, Phys. Rev. B $\underline{19}$, 6094 (1979); T. L. Loucks, *Augmented Plane Wave Method* (Benjamin, New York, 1967); O. K. Andersen, Phys. Rev. B $\underline{12}$, 3060 (1975).

[17]W. Eberhardt, G. Kalkoffen, C. Kunz, D. E. Aspnes, and M. Cardona, Phys. Status Solidi B $\underline{28}$, 135 (1978).

[18]M. Aono, F. J. Himpsel, and D. E. Eastman, unpublished.

[19]D. A. Shirley, R. L. Martin, S. P. Kowalcsyk, F. R. McFeely, and L. Ley, Phys. Rev. B $\underline{15}$, 544 (1977).

[20]J. F. van der Veen, F. J. Himpsel, P. Heimann, and D. E. Eastman, private communication.

[21]P. S. Ho, G. W. Rubloff, J. E. Lewis, V. L. Moruzzi, and A. R. Williams, in *Proceedings of the Symposium on Thin Films and Interfaces*, edited by John E. Baglin and John M. Poate (Electrochemical Society, New York, 1980), PV 80–2, 85.